# DESIGN TOOL FOR DISCONTINUOUS RESIN PATTERNS IN VACUUM BAG-ONLY PREPREGS

# Sarah G.K. Schechter, Timotei Centea, Steven Nutt University of Southern California

## **ABSTRACT**

Discontinuous resin distributions facilitate transverse air removal in vacuum bag-only prepregs during out-of-autoclave processing, and enable robust manufacturing. Methods to create discontinuous resin distributions with various pattern types and feature sizes have been demonstrated in recent reports. However, this new capability has expanded the design space for prepreg manufacturing, and optimum pattern characteristics have not been identified. In this work, a geometric model was developed to simulate prepregs and laminates with discontinuous resin distributions of various pattern type, feature size, stacking orientation, and ply count. Key metrics were employed to explore the capacity for air evacuation at room temperature. In particular, the projected surface area exposed was calculated to examine the fraction of uninhibited transverse air evacuation pathways. Secondly, sealed interfaces corresponding to the percentage of closed interlaminar regions within laminates were estimated. Finally, the tortuosity (the ratio of actual average gas transport path to straight-line path) of the dry pore network was calculated. A full factorial design, analyzed by *n*-way ANOVA and multi-comparison tests, was conducted to reveal the aspects of prepreg designs having the greatest influence on these metrics. Finally, these insights were used to fabricate prototype prepregs and experimentally measure their transverse permeability. Results revealed that a large number of sealed interfaces and high tortuosity were associated with lower permeability, indicating that these metrics can be used to screen resin patterns using the developed model. Broadly, the results validated a methodology to differentiate between discontinuous resin patterns with regards to air evacuation of the prepreg at room temperature, and therefore reduce the design space. Ultimately, this work can be used to guide prepreg design and to support manufacturing of high-quality composites by out-ofautoclave methods.

#### 1. INTRODUCTION

An increasingly viable alternative to conventional autoclave manufacturing methods is the use of out-of-autoclave (OoA) vacuum-bag-only (VBO) prepregs [1]. Problems associated with autoclave use include high capital and operational costs of the pressure vessels, size limits, and limited throughput. While these issues are alleviated by VBO prepregs, OoA/VBO processing is often insufficient to reduce porosity to acceptable levels because the consolidation pressure is limited to 0.1 MPa (1 atm). Thus, VBO-cured parts can exhibit porosity and diminished mechanical properties when trapped gases are not evacuated during early stages of processing [1].

Conventional VBO prepregs are constructed by pre-impregnating the fiber bed using a hot-melt process. Pre-catalyzed resin is formed into a thin film on backing paper and pressed onto the fiber bed using rollers [2]. The resulting prepreg is designed to have dry, highly permeable gas evacuation pathways at the mid-plane of the ply. These pathways can be sufficient to achieve

low defect levels within cured parts when combined with appropriate consumables, such as edgebreathing dams [2]. However, under sub-optimal conditions, such as inadequate vacuum, high levels of absorbed moisture in the resin, or part geometries that prevent in-plane air removal, laminates fabricated from conventional VBO prepregs can lead to unacceptable void levels [1].

# 1.1 Background

Studies have shown that discontinuous resin films increase the capacity for transverse air evacuation by creating additional egress pathways [3–5]. These pathways can virtually eliminate porosity caused by entrapped gases and low-pressure VBO consolidation. For example, Roman showed that the resultant cured composite parts using prepreg with discontinuous resin film exhibited near-zero internal porosity. Grunenfelder et al. showed that even under non-ideal manufacturing conditions, a discontinuous prepreg format (denoted USCpreg) produced near-zero internal porosity and no surface defects. Tavares et al. measured the transverse air permeability at room temperature and processing conditions of a commercial semipreg ("Zpreg") and an equivalent unidirectional prepreg constructed with continuous resin. The permeability of the semipreg was three orders of magnitude greater than the continuous film prepreg before and during the cure cycle. This increase in permeability arises from a network of dry interconnected pore spaces. These collected works demonstrate the value of producing laminates from prepreg with discontinuous resin. Nevertheless, methods of production allowing for the creation of arbitrary patterns on a chosen fiber bed were not identified nor disclosed.

Previously, we demonstrated a simple technique via polymer dewetting on a substrate to create discontinuous resin patterns [6,7]. To create an array of nucleation sites, resin film was perforated on silicone-coated backing paper (the substrate). When heated, the resin film recedes at the perforated sites (nucleating dewetted openings). Finally, the dewetted resin was transferred onto the fiber bed by pressing briefly. Finely tuned patterns of various shapes and sizes can be made using this technique. Regardless of the architecture, the patterned resin films created using this technique can be applied to any fiber bed.

# 1.2 Objectives

Polymer film dewetting allows for the creation of resin distribution patterns with varying shapes and sizes. However, with this capability, the design space has been substantially enlarged, and the optimal patterns for efficient air evacuation is not obvious nor has it been identified. In addition, the relationships between pattern characteristics, laminate design, and prepreg properties with regards to transverse air evacuation are unclear. Experimental screening based on prepreg production, laminate layup, and permeability testing will be arduous, time-consuming, and ineffective in highlighting governing trends. The present work focused on developing a method to differentiate between continuous resin patterns without excessive experimentation or set-up time, and identify prepreg characteristics that likely favor rapid transverse air evacuation in the initial state (at room temperature, before significant flow-compaction has occurred). A MATLAB program was developed to accomplish these objectives, which generated geometric models of the prepreg (in 2D) and of an arbitrary laminate (in 3D). Several attributes from these models were measured: projected surface area exposed of the stacked prepreg, sealed interfaces, and tortuosity of the air evacuation pathways. Then, to determine the effect of pattern factors on each of these attributes, a factorial design study was conducted. Multi-comparison tests and nway ANOVA were used to analyze the factorial design. Laminates were selected for

experimental validation from the results from the multi-comparison tests. The effective air permeability at room temperature of these laminates was tested. The study effectively outlines a methodology that can readily discriminate between prepreg designs and allow for the selection of prepregs that efficiently evacuate air.

#### 2. MODELING

## 2.1 Model Development

Creating a method for rapidly screening prepreg configurations and resulting laminates with respect to initial capacity for transverse air evacuation at room temperature was the primary goal of this modeling. In this first attempt, explicitly modeling resin flow and fiber bed compaction for an arbitrary discontinuous prepreg was excluded from the scope. Different approaches, including geometric analysis (employed here), analytical models of flow in porous media, and computational simulations based on finite element methods, can be used to estimate the capacity for gas flow within complex-shaped porous media. Valuable insights into underlying physics can be provided by these analytical models, and such models have been used to generate process maps to guide material and process development [8]. Computational models allow detailed, often multi-physics analysis of physical phenomena within complex domains [9]. However, both methods must be configured and solved for specific domain geometry. While parameterization of scales is possible, neither option is inherently well suited to broad, rapid screening of arbitrary prepreg and laminate patterns. For these reasons, this study focused on investigating the viability of a geometric model that is simple to implement (parametric) and execute. Ultimately, the model can be used to reduce a large design space to a small subset of potential solutions, which can be evaluated experimentally.

Simplifying assumptions were relied on during model development. Gas transport occurs much faster through dry regions (unsaturated fiber reinforcement) than through saturated regions [3,4]. Hence, the model was based on the premise that gas evacuation capacity is primarily governed by characteristics (size and connectivity) of the dry pore network (rather than by bubble migration through resin). Therefore, void growth and transport within the fluid domain were not modeled. Following initial compaction, the microstructure of partially-impregnated prepregs does not evolve substantially under room temperature vacuum compaction [10]. For this reason, a rigid geometric framework was employed for the model, without simulating compaction. Furthermore, the thickness of a resin layer and a fiber layer were arbitrarily defined and remained constant across prepreg designs. However, in actuality, as the resin feature dimensions decrease, the thickness of the resin layer must increase.

# 2.2 Parametric Study

## 2.2.1 Methods

Placing a continuous layer of resin film on either or both sides of a fiber bed [Fig. 1a] generally produces prepregs. Usually, in OoA prepregs, the resin partially impregnates the fiber bed, where the dry space allows for in-plane evacuation of air at the ply mid-plane. OoA prepreg formats with discontinuous resin feature surface openings that allow for additional air evacuation in the transverse direction [Fig. 1b]. Stacking plies of prepreg constructs a laminate. The placement of the resin on the fiber bed and the plies of the prepreg for a laminate are random (no intentional alignment of features). Air can be readily entrapped in the space between the resin layers of the

stacked prepregs (the interface). Furthermore, with discontinuous resin, this interface can either be sealed, if surface openings are too small, or not sealed, allowing for an interconnected evacuation pathway in the transverse direction.

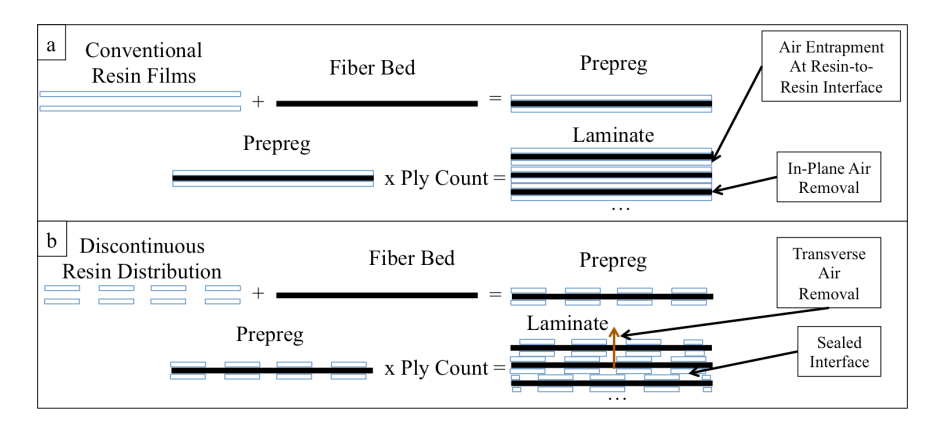


Figure 1. (a) The conventional fabrication of prepreg and laminates with continuous resin films, which illustrate air entrapment at the resin-to-resin interface and the mechanism of air removal in the in-plane direction. (b) The creation of prepreg and laminates with a discontinuous resin distribution, which illustrate air removal in the transverse direction and the potential for seal-off between resin layers (due to small surface openings and random placement during stacking).

The code was written to create patterns that replicate those that were created by the polymer film de-wetting technique [6,7]. These patterns included stripes, islands, and grids [Fig. 2a]. To create these patterns, a four-element vector of the form  $[x\ y\ w\ h]$  was used to create rectangles in 2D coordinates. The location is determined by the x and y elements, and the size is determined by the w and h elements. Curvature was also specified, where no curvature is a value of 0, and maximum curvature is a value of 1. For stripes, the curvature of the rectangle was set to 0, whereas for islands and grids, the curvature was set to 1. The islands and grid patterns were programmed to be mutually reciprocal by computing the complement of the image. Furthermore, to eliminate any automatically created borders, the images were cropped to the same size. Examples of a single resin ply created by this method for each of the three pattern types studied are shown in Fig. 2b. The black regions represent void space (a pixel intensity of 0), whereas white regions represent the resin (a value of 1).

The code was designed so that the laminate was symmetrical about the midpoint. Therefore, at the midpoint, the resin layers are orientated in the same direction. Each resin layer was randomly translated in the x- and y-directions by generating a single uniformly distributed random number in the interval (0,1). This random number was multiplied by the phase, which was the sum of the resin distance and the dry space distance. Then this number is added to the location elements in the four-element vector.

Three key output attributes were defined to generate a broad description of the air evacuation capacity of a laminate constructed with discontinuous resin patterns: (a) the 2D projected surface area exposed, (b) the percentage of sealed interfaces (relative to the total number of inter-ply regions), and (c) the tortuosity of the dry pore network pathways. The presence and amount of direct unobstructed transverse-oriented pathways are described by the 2D projection of the exposed surface area. However, gases can move in the transverse direction by migrating laterally

through the dry fibers even with zero projected surface area exposed. Thus, the number of interruptions in the modeled pore network for flow in the transverse direction is described by the percentage of sealed interfaces. Finally, the distance gas would have to travel within the laminate to escape (assuming no sealed interfaces) is described by the tortuosity measurements. Large tortuosity values were expected to reduce the momentum for gas flow, therefore reducing permeability, even in the absence of sealed interfaces.

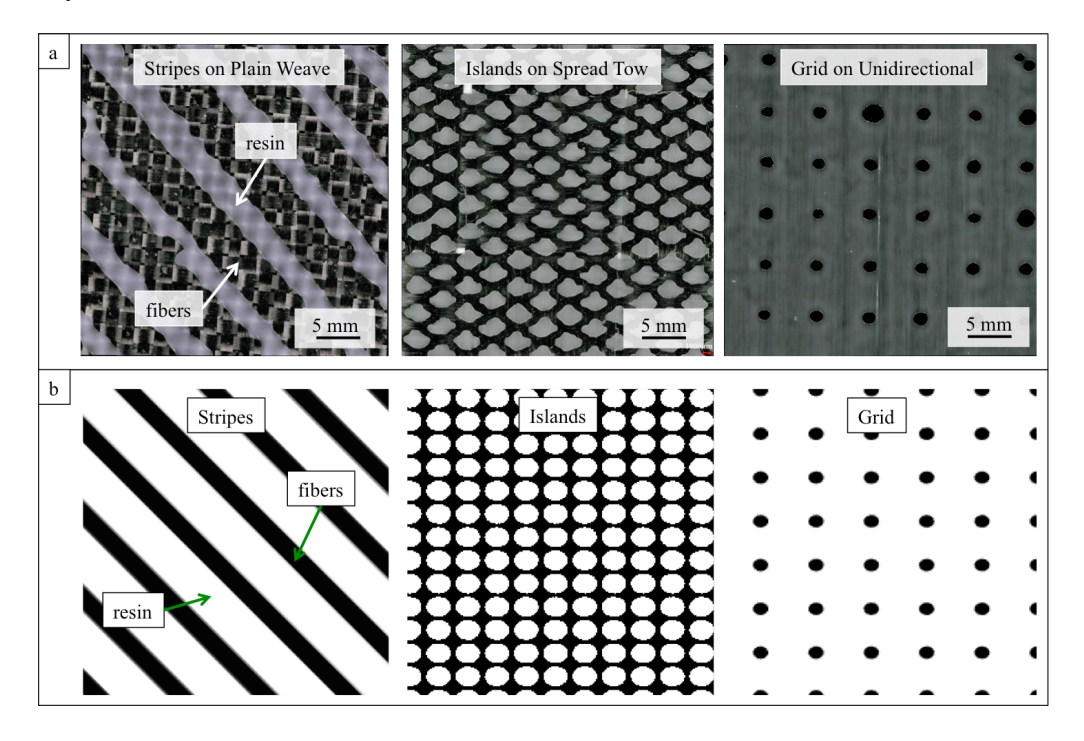


Figure 2. (a) Example of the discontinuous resin patterns created via the polymer film dewetting technique. (b) Examples of the discontinuous resin patterns coded in the MATLAB program.

An average value for each parameter measurement was achieved by iterating 25 times. The resin layers are randomly placed on the fiber bed when prepreg and laminates are manufactured. Thus, the iterations would compensate for the randomness in making prepregs and laminates. The parameters were measured for 4, 8, and 16 plies. Three orientations were programmed for measurements, which were  $[0/0]_n$ ,  $[0/90]_n$ , and  $[0/90/\pm45]_n$ .

Fig. 3 illustrates the code for the three parameters. For calculations of projected surface area exposed, the laminates (or "stacks") were created by matrix addition of the appropriate number of resin layers according to the target ply count. The surface area exposed,  $A_{SE}$ , then was calculated by dividing the number of nonzero elements by the number of total elements.

For sealed interfaces calculations, an interface was created by the matrix addition of two resin layers. The number of interfaces created for each laminate was 3 for 4 plies, 7 for 8 plies, and 15 for 16 plies. Eqn. 1 was used to calculate the exposed surface area of the interface. A threshold value of 0.1 % was employed, where the interface was considered sealed if the surface area exposed was less than 0.1 %. The percentage of sealed interfaces was calculated by dividing the average number of sealed interfaces by the total number of interfaces.

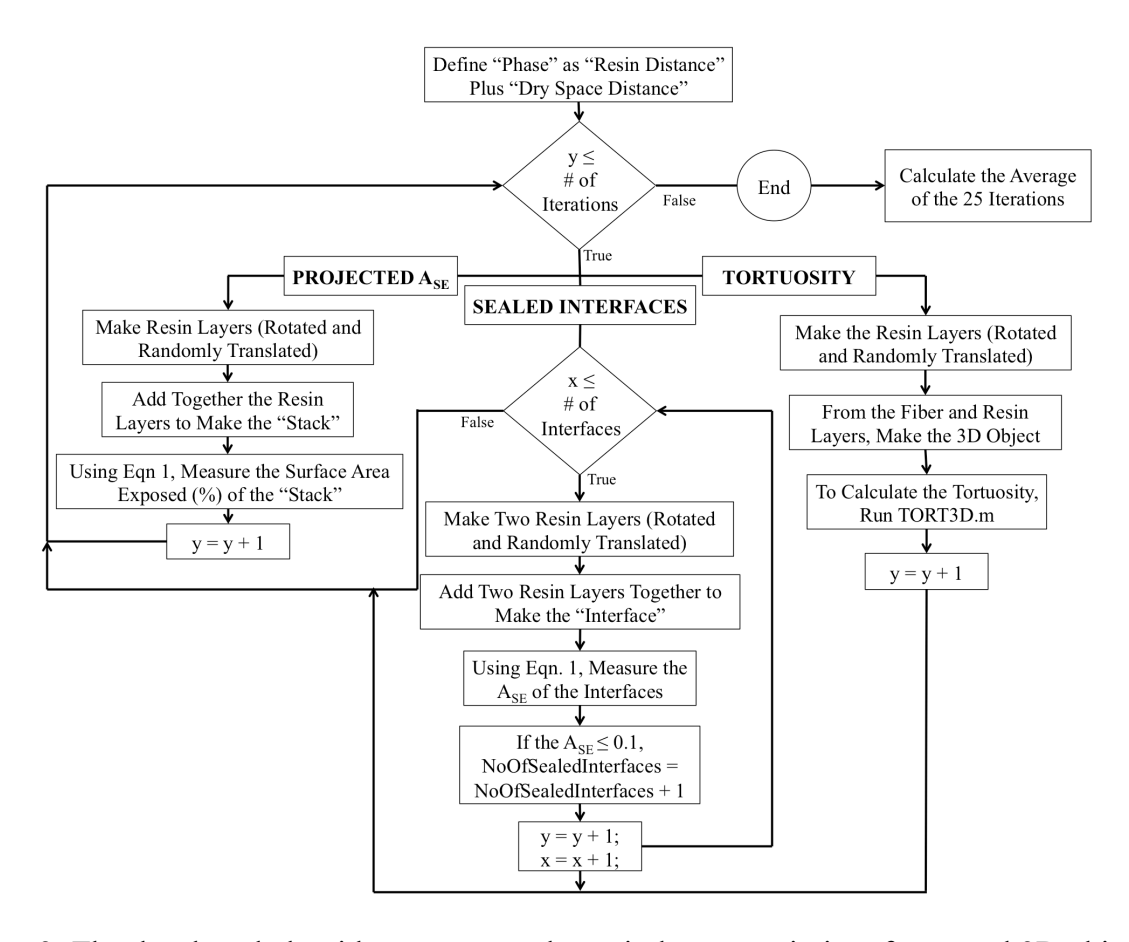


Figure 3. The developed algorithms to create the resin layers, resin interfaces, and 3D objects to compute the projected surface area exposed, sealed interfaces, tortuosity, respectively.

For tortuosity calculations, 3D objects were created to represent the laminates fabricated with discontinuous resin. The fiber layer consisted of a matrix of all zeroes. The resin layers were constructed just as before, in that the layers were rotated and randomly translated. Each fiber layer was composed of four layers, and each resin layer was composed of two layers. Fig. 4 shows examples of how the 3D objects were rendered. Next, the TORT3D.m program [11] was used to measure the tortuosity of the transverse air evacuation pathways. A segmented image was read by the code and all possible tortuous pathways were determined in order to compute tortuosity. Utilizing the medial surface of the void space, a guided search for the connected path in the void space of the image was conducted by the algorithm. To compute tortuosity, the average of all connected pathways in that direction was used. Geometric tortuosity,  $\tau_g$ , was defined as:

$$\tau_g = \frac{\langle L_g \rangle}{L_s} \tag{1}$$

where  $\langle L_g \rangle$  is the average length of true paths through the porous media and  $L_s$  is the length of the straight-line path across the porous media in the direction of flow. The tortuosity value,  $\tau$ , acquired from the code was defined as:

$$\tau = \frac{\sum_{i=1}^{n} l_{p_i}}{n} \tag{2}$$

where  $l_p$  is the given path through the void space that connects the boundary of the images in the direction of flow,  $l_s$  is the corresponding straight line, and n is the number of paths. The program returned a tortuosity value of "NaN" if the 3D object contained a sealed interface.

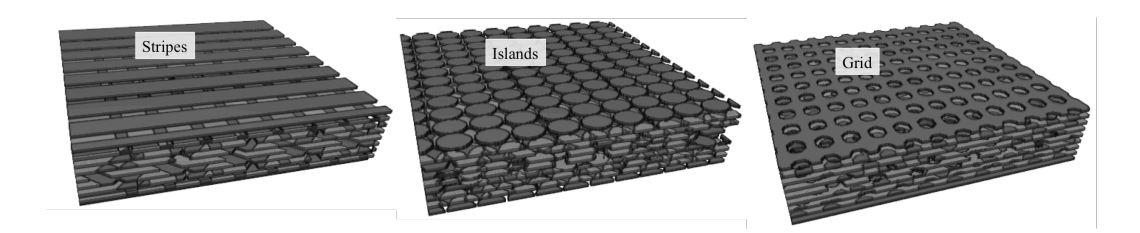


Figure 4. Examples of the 3D objects coded, which represent laminates with discontinuous resin patterns. Each object was 8 plies,  $[0/90/\pm45]_n$ , and 30 % single layer surface area exposed.

## 2.2.2 Results

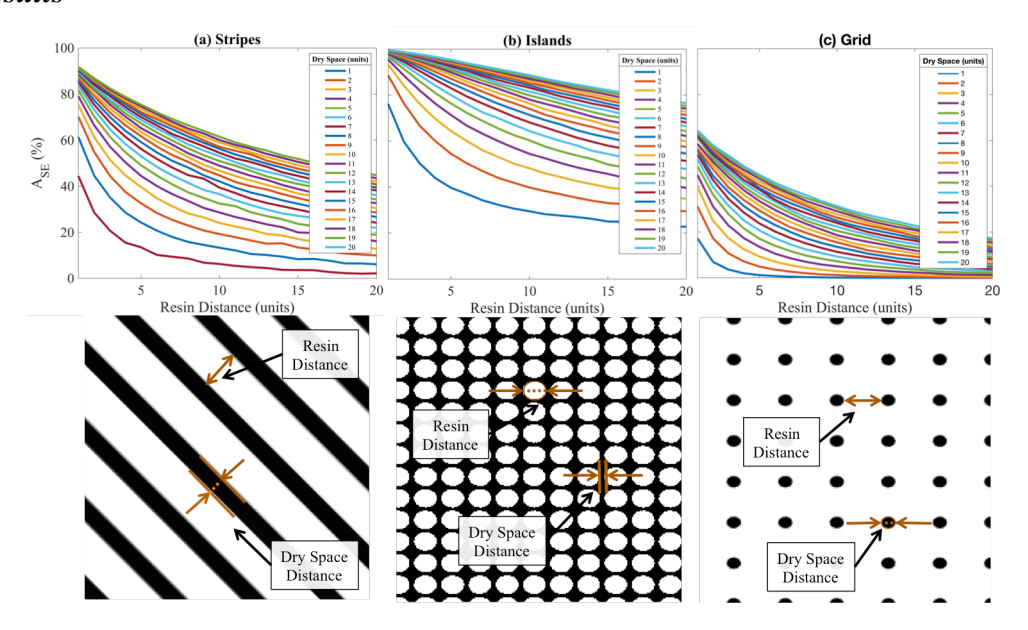


Figure 5. Surface area exposed for a single resin layer for each of the studied patterns [(a) stripes, (b) islands, (c) grid] with the range of resin and dry space distances of 1 to 20. Diagrams of the variables "Resin Distance" and "Dry Space Distance" are below each graph.

Single Layer  $A_{SE}$ . The exposed surface area [Eqn. 1] of a single discontinuous resin film was measured for all three patterns for resin widths or diameters specified between 1 and 20, and dry space distance specified between 1 and 20 [Fig. 5]. The limitations of the amount of initial surface area exposed are shown in the graphs of Fig. 5a-c. The largest range of exposed surface area was yielded by the stripes patterns [Fig. 5a], with values from 10 % - 90 %. However, for

the stripes pattern, an upper limit of 90 % does appear to exist. For the islands pattern [Fig. 5b], no upper limit appeared to exist, but a lower limit of 15 % did manifest. For the grid pattern [Fig. 5c], an upper limit of 65 % did exist, however no lower limit existed. The range of surface area exposed that could be used for comparison between the three patterns was 15 % - 65 %, where all three constraints are considered.

Projected  $A_{SE}$ . As each resin layer was added to the stack, the projected surface area exposed was measured. These measurements were performed for single layer surface area exposed values of 30 % and 60 %. The projected surface areas exposed of the three patterns (stripes, islands, and grid) are compared in Fig. 6a. The decrease in the projected surface area exposed was the same across the pattern types provided the single layer surface area exposed value was the same. The projected surface area exposed for the stripes pattern oriented in  $[0/0]_n$ ,  $[0/90]_n$ , and  $[0/90/\pm 45]_n$  are compared in Fig. 6b. Orientation had a negligible effect on the behavior of how the projected surface area exposed decreased. The point where the projected surface area exposed approached zero is also shown on these graphs. For 30 % single layer surface area exposed, the projected surface area exposed was nearly zero after just 2 plies (4 resin layers). For 60 % single layer surface area exposed, the projected surface area exposed, the projected surface area exposed was nearly zero after 5 plies (10 resin layers) are laid down.

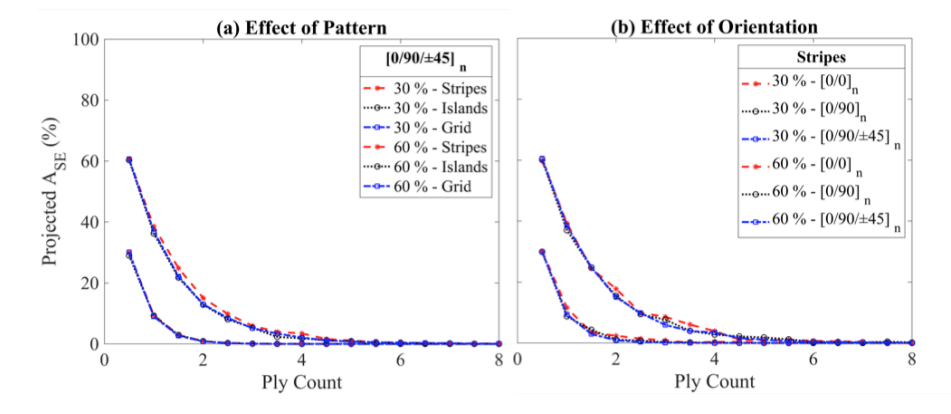


Figure 6. Graphs are selected results of the projected surface area exposed [(a)  $[0/90/\pm45]_n$  (b) Stripes] as ply count increases from the code developed.

Sealed interfaces. The percentage of sealed interfaces was calculated for 16-ply laminates with values of single layer surface area exposed between 7.5 % and 60 %. The sealed interfaces across the three patterns (stripes, islands, and grid) with an orientation of  $[0/0]_n$  are compared in Fig. 7a. At values less than 60 %, the stripes pattern resulted in substantial amounts of sealed interfaces (10.1 % - 87.2 %). At values less than 45 %, the grid pattern also produced substantial amounts of sealed interfaces (9.9 % - 61.1 %). On the other hand, islands only yielded sealed interfaces at values less than 30 %. However, the sealed interfaces could not be measured at 7.5 % since an islands design with this value could not be obtained.

The number of sealed interfaces for 16-ply laminates laid up with stripes in each of the three orientations ( $[0/0]_n$ ,  $[0/90]_n$ , and  $[0/90/\pm45]_n$ ) is compared in Fig. 7b. Intuitively, stripes would appear to be the most sensitive of the three patterns to orientation. The data shows that  $[0/90]_n$  and  $[0/90/\pm45]_n$  laminates behaved identically, where the proportion was markedly less than for  $0/0]_n$ . Intuitively, laminates produced with resin stripes oriented in either  $[0/90]_n$  and  $[0/90/\pm45]_n$ 

should not exhibit any sealed interfaces because the stripes are orthogonal. However, the stacking was symmetric (the stripes were parallel) at the midpoint), which could cause a sealed interface in certain cases of the randomly oriented set.

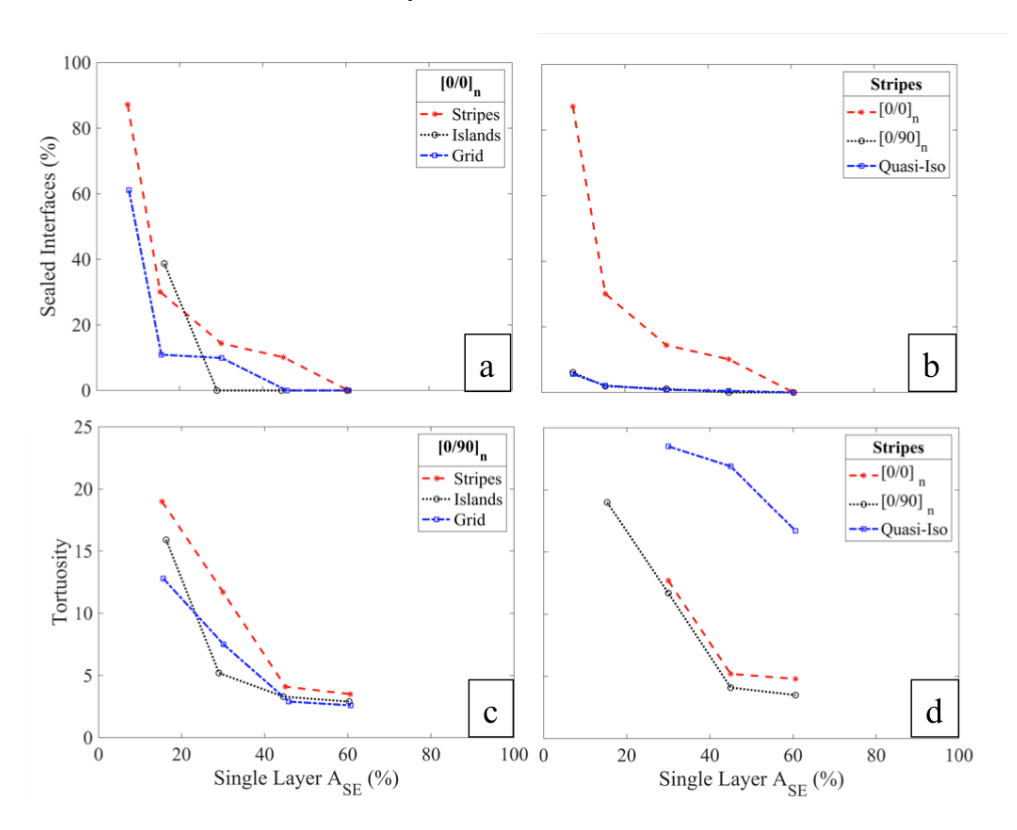


Figure 7. Graphs are selected results of sealed interfaces [(a)  $[0/0]_n$  (b) Stripes] and tortuosity [(c)  $[0/90]_n$  (d) Stripes] measurements from the code developed for 16 ply laminates.

Tortuosity. Tortuosity (a unitless quantity) was measured for 16-ply laminates. These laminates stacked in the orientation of  $[0/90]_n$  for stripes, islands, and grid are compared in Fig. 7c. On average, the stripes had greater tortuosity than either the island or grid patterns. The island and grid patterns behaved similarly with high single layer surface areas exposed. The 16-ply stripes laminates oriented in  $[0/0]_n$ ,  $[0/90]_n$ , and  $[0/90/\pm45]_n$  are compared in Fig. 7d. On average, the  $[0/90]_n$  laminate had a smaller tortuosity. However, the  $[0/90/\pm45]_n$  laminate resulted in unusually high tortuosity. The fact that each ply of a laminate produced with a quasi-isotropic stacking orientation was oriented in a different direction can be attributed to the reason for high tortuosity. These different orientations would result in more indirect and convoluted pathways than a simpler orientation like  $[0/0]_n$  and  $[0/90]_n$ .

#### 2.3 Statistical Analysis

A full factorial experiment consists of two or more factors, each with discrete possible values, where the experimental values take on all possible combinations of these levels across all such factors [12]. Evaluation of the effects of each factor on the response variable is accomplished by such an experiment, as well as the importance of interactions between factors on response. Here, each experiments (for each response variable) was denoted as a 3<sup>4</sup> factorial, which identifies the number of factors (4), the number of levels each factor has (3), and the number of experimental

conditions in the design ( $3^4 = 81$ ). Three response variables were being measured: projected surface area exposed, sealed interfaces, and tortuosity. Thus, the total number of conditions was 243 (3 x 81). The four factors (with the three levels) studied were pattern type (stripes, islands, grid), single layer surface area exposed (30 %, 45 %, 60 %), ply count (4, 8, 16), and stacking orientation ( $[0/0]_n$ ,  $[0/90]_n$ , and  $[0/90/\pm 45]_n$ ).

Table 1. Summary of the *n*-way ANOVA results for measurements of (a) the Projected Surface Area Exposed, (b) Sealed Interfaces, and (c) Tortuosity.

Variable	Sum Sq.	df	Mean Sq.	F	Prob > F
Projected A <sub>SE</sub> (%)					
Single Layer A <sub>SE</sub> (%)	22.8	2	11.4	478.8	4.4e-35
Ply Count	23.5	2	11.7	493.5	2.0e-35
Orientation	1.6	2	0.8	32.7	4.9e-10
Single Layer A <sub>SE</sub> (%) * Ply Count	38.5	4	9.6	404.9	1.5e-39
Single Layer A <sub>SE</sub> (%) * Orientation	2.8	4	0.7	29.1	6.7e-13
Ply Count * Orientation	2.2	4	0.6	23.4	3.0e-11
Single Layer A <sub>SE</sub> (%) * Ply Count * Orientation	3.9	8	0.5	20.3	9.3e-14
Sealed Interfaces (%)					
Pattern	113.4	2	56.7	28.6	3.4e-9
Single Layer A <sub>SE</sub> (%)	181.5	2	90.7	45.8	2.3e-12
Orientation	245.4	2	122.7	61.9	1.1e-14
Pattern * Single Layer A <sub>SE</sub> (%)	119.8	4	30.0	15.1	2.4e-8
Pattern * Orientation	138.1	4	34.5	17.4	3.1e-9
Single Layer A <sub>SE</sub> (%) * Orientation	198.0	4	49.5	25.0	9.6e-12
Pattern * Single Layer A <sub>SE</sub> (%) * Orientation	179.2	8	22.4	11.3	3.1e-9
Tortuosity					
Pattern	458.2	2	229.1	283.1	0
Single Layer A <sub>SE</sub> (%)	428.6	2	214.3	264.8	0
Ply Count	33.5	2	16.7	20.7	0
Orientation	764.6	2	382.3	472.3	0
Pattern * Single Layer A <sub>SE</sub> (%)	88.0	4	22.0	27.2	0
Pattern * Ply Count	48.0	4	12.0	14.8	0
Pattern * Orientation	494.9	4	123.7	152.9	0
Single Layer A <sub>SE</sub> (%) * Ply Count	24.5	4	6.1	7.6	2.0e-4
Single Layer A <sub>SE</sub> (%) * Orientation	102.6	4	25.7	31.7	0
Ply Count * Orientation	44.5	4	11.1	13.8	0
Pattern * Single Layer A <sub>SE</sub> (%) *Orientation	56.2	8	7.0	8.7	0
Pattern * Ply Count * Orientation	18.8	8	2.4	2.9	1.5e-2

Analysis of Variance (ANOVA) was used to analyze the factorial experiment responses. ANOVA is a collection of statistical models, and their associated estimation procedure is used to analyze the differences amongst group means in a sample [12]. In its simplest form, ANOVA provides a statistical test of whether the population means of several groups were equal, and therefore generalize the t-test to more than two groups.

Calculated from the null hypothesis and the sample, a test result was treated as statistically significant if it was deemed unlikely to have occurred by chance (assuming the truth of the null hypothesis). A statistically significant result (p-value  $\leq 0.05$ ) justified the rejection of the null hypothesis (all groups were random samples from the same population). Thus, rejecting the null hypothesis signified that the difference in observed effects between treatment groups was

unlikely to be random chance.

A 4-way ANOVA was initially performed for each experiment. However, elements often would have missing *p*-values (represented as "NaN"), which indicated missing factor combinations and/or that the model has higher-order terms. Therefore, a 3-way ANOVA was performed instead, which allowed for the identification of statistically insignificant terms. These terms were then omitted, where their effects were pooled into the error term. Without the statistically insignificant terms, the *n*-way ANOVA was then performed again. Table 1 presents the ANOVA results for each response variable.

For surface area exposed, only three of the factors had a p-value  $\leq 0.05$ : single layer surface area exposed, ply count, and orientation. This result signified that the projected surface area exposed was insensitive to the pattern type. Ply count and single layer surface area exposed had the largest F-values, which indicated that these two variables were the most influential on projected surface area exposed. The F-value is defined as ratio of the variation between sample means to the variation within the samples, where the null hypothesis was that these two variance values were roughly equal (F-value = 1). Thus, the greater the relative variance among the group means, the larger the F-value (the p-value indicates the probability of obtaining an F-value as extreme or more extreme than the one observed under the assumption that the null hypothesis was true).

For sealed interfaces, the ANOVA results indicated that all factors except ply count were significant, whereas, for tortuosity, all factors were significant. Therefore, the number of plies of prepreg in a laminate has no effect on the percentage of sealed interfaces, but ply count did affect tortuosity. The stacking orientation had the largest *F*-value for both the sealed interfaces and tortuosity. The significance of the orientation may have been heavily skewed by its effect on the stripes pattern, which was the most sensitive to orientation.

For the 2D projected surface area exposed, the pattern type was determined to be insignificant, so the results were pooled together without regard to pattern type. The 4-ply laminates made with 60 % single layer surface area exposed and oriented  $[0/0]_n$  was the group with the largest mean (and being significantly different from the rest). The next two largest (significantly different) means, in order, were the same 4-ply laminates with 60 % single resin surface area exposed, but oriented  $[0/90]_n$  and  $[0/90/\pm 45]_n$ . These conditions identified prepreg designs with the highest quantity of uninhibited air evacuation pathways in comparison to the other conditions tested (4 plies, 60 %  $A_{SE}$ ,  $[0/0]_n$ ). However, all three conditions were for 4-ply laminates, indicating that uninhibited air evacuation pathways did not exist for larger ply counts.

For sealed interfaces and tortuosity, ply count was pooled, because it was insignificant from the n-way ANOVA results. For sealed interfaces, three laminates exhibited the largest (significantly different) means, where all three were oriented  $[0/0]_n$ . Two of the laminates were stripes with 30 % and 45 % surface area exposed, while the third laminate was a grid with 30 % surface area exposed. These results indicated prepreg designs that would result in large amounts of sealed interfaces (stripes, 30 % or 45 %  $A_{SE}$ ,  $[0/0]_n$  and grid, 30 %,  $[0/0]_n$ ). For tortuosity, the striped pattern with 30 % surface area exposed and stacked in a  $[0/90/\pm45]_n$  orientation is associated with the largest mean. These results indicated a prepreg design that would result in high tortuosity (stripes, 30 %  $A_{SE}$ ,  $[0/90/\pm45]_n$ ). These multi-comparison results will be demonstrated in experimental verification testing, described next.

#### 3. EXPERIMENTS

Experiments were performed to verify if geometric modeling could discriminate between prepregs with low and high room temperature transverse gas permeability, and determine which output attributes were most closely correlated to effective permeability.

#### 3.1 Materials

A toughened epoxy resin (PMT-F4A, Patz Materials & Technology, California, USA) and a unidirectional non-crimp fiber bed (Fibre Glast Development Corporation, Ohio, USA) were selected for testing. The epoxy resin featured medium-to-dry tack, and the film weight was 152 g/m² (gsm). The fabric thickness was 0.36 mm, and the weight was 305 gsm. The tape exhibited negligible crimp, except around the binder threads. The binder threads are polyester fill threads stitched in one direction, which held the unidirectional fibers in place. The fabricated prepreg yielded a resin content of 50 % by weight, which was much larger than standard unidirectional prepreg (33 %). The thick resin was used to ensure that the dewetting process resulted in features that were close to the model image. At thinner thicknesses, the resin will dewet at surface imperfections, such as tears or depressions. The resin had been stored in a freezer for 6 months and had accumulated 1 week of out-life. (The storage life of this resin was 2 years at -10 °C. The out-life was 120 days at room temperature.)

Dewetting was executed as described previously [6,7]. Nucleation sites were created using a box cutter to facilitate dewetting. The dewetting was carried out on silicone-coated release paper. For the dewetting, the films were heated by a standard oven (Blue M Oven, Thermal Product Solutions, Pennsylvania, USA).

## 3.2 Permeability

The effective slip-corrected transverse permeability was measured for 8 plies of prepregs produced using the stripes pattern, with 30 % surface area exposed for each of the orientations ([0/0]<sub>n</sub>, [0/90]<sub>n</sub>, and [0/90/±45]<sub>n</sub>). These conditions were chosen to determine how sealed interfaces and tortuosity affected transverse air evacuation. The case of a large amount of sealed interfaces and a small tortuosity is represented by the orientation [0/0]<sub>n</sub>. The opposite case, where the amount of sealed interfaces was small and the tortuosity was large, is represented by the orientation [0/90/±45]<sub>n</sub>. On the other hand, the orientation [0/90]<sub>n</sub> represented the case where both sealed interfaces and tortuosity were small. Fig. 8a summarizes the values for sealed interfaces and tortuosity for each of these prepregs. Since the results indicated that only ply count and single layer surface area exposed affected projected surface area exposed, this parameter was not tested. In a manufacturing setting, ply count is a specification that cannot be manipulated. In addition, a change in feature dimensions would undoubtedly change the values for the number of sealed interfaces and tortuosity.

To expand the permeability data set to encompass other pattern types and feature dimensions, samples from a previous report [6,7] were also included. These samples included both a grid pattern and a  $[0/90]_n$  stacking orientation. The single layer surface area exposed for each sample was either 13 % or 50 %. The prepreg with 13 % exposed surface area was likely to have a large number of sealed interfaces (on average 11 %) and tortuosity air evacuation pathways. On the other hand, the prepreg with 50 % exposed surface area was likely to have no sealed interfaces (0

%) and less tortuous air evacuation pathways.

Following the falling pressure method described by Kratz et al. [13] and Tavares et al. [14], a custom test fixture was used for the experiments [13]. Supported by stacks of honeycomb core, the plies of prepreg were laid over a cavity of known dimensions. To permit air evacuation only in the z-direction, the edges of the laminates were sealed with vacuum tape, which prevents edge breathing. The laminates were covered with perforated release film and breather, and then vacuum-bagged. Drawing vacuum in the bag created a pressure difference between the core cavity and the bag. Using data acquisition software (LabVIEW, National Instruments) with a pressure transducer, the evolution of pressure in the cavity was monitored. The measurements were used to estimate an effective permeability coefficient. These tests were executed at room temperature (20 °C).

Two replicates were tested for each configuration, with a minimum of three pressure decay trials per sample, to obtain an average permeability value. Each trial was conducted till the time at which the cavity pressure stabilized, which indicated that the flow had ceased. The configuration was then re-pressurized to begin the next trial. Since air evacuates more quickly when the configuration had not been previously compacted, the data from the first trial was omitted.

Using Darcy's Law, the 1D laminar flow of compressible air at isothermal and adiabatic conditions through a porous medium [13] can be described by

$$\frac{-KAP_{Bag}}{L\mu V_{Core}} = \ln \left[ \frac{(P_{Core}(0) + P_{Bag})(P_{Core}(t) - P_{Bag})}{(P_{Core}(0) - P_{Bag})(P_{Core}(t) + P_{Bag})} \right]$$
(3)

where K is the permeability scale in the flow direction in  $m^2$ , A is the cross-sectional area (1.46 x  $10^{-2}$  m<sup>2</sup>),  $P_{Bag}$  is the pressure at the bag side (5 x  $10^3$  Pa),  $P_{Core}$  is the pressure at the honeycomb core side in Pa, L is the lateral dimension in m,  $\mu$  is the viscosity of air at room temperature (1.85 x  $10^{-5}$  Pa\*s), t is time in s, and  $V_{Core}$  is the volume of the core (7.87 x  $10^{-4}$  m<sup>3</sup>). Here, the vacuum level was assumed to be 95 %, which corresponds to an absolute vacuum bag pressure of 5 kPa. Plotting the left-hand side versus t yields a straight-line plot. The slope can be used to determine the effective air permeability of the prepreg, K.

Fig. 8b presents a summary of the permeability values of the laminates and a plane created by a linear regression fit of the data. Displayed on the graph is the equation for the linear regression model and the coefficient of determination ( $R^2$ ). Sealed interfaces and tortuosity was defined by the symbols  $n_{sealed}$  and  $\tau$ , respectively. The value for  $R^2$  was 0.966, which indicates that the model fits the data. The planar fit indicated that an increase in the percentage of sealed interfaces and the tortuosity does indeed decrease the transverse permeability of the prepregs, which is a less desirable outcome for robust manufacturing. The equation indicated that the percentage of sealed interfaces had a larger effect on the decrease in permeability than did tortuosity.

The experimental results demonstrate that the prepreg and laminate features included in the study contribute to the efficiency with which prepregs evacuate air and other gases. Furthermore, these results also indicated the aspects of the prepreg design which have the greatest effect on this efficiency. Notably, sealed interfaces had a much greater effect on air permeability than tortuosity. The methodology and results described here can be used to guide the design of

discontinuous resin patterns for VBO prepregs.

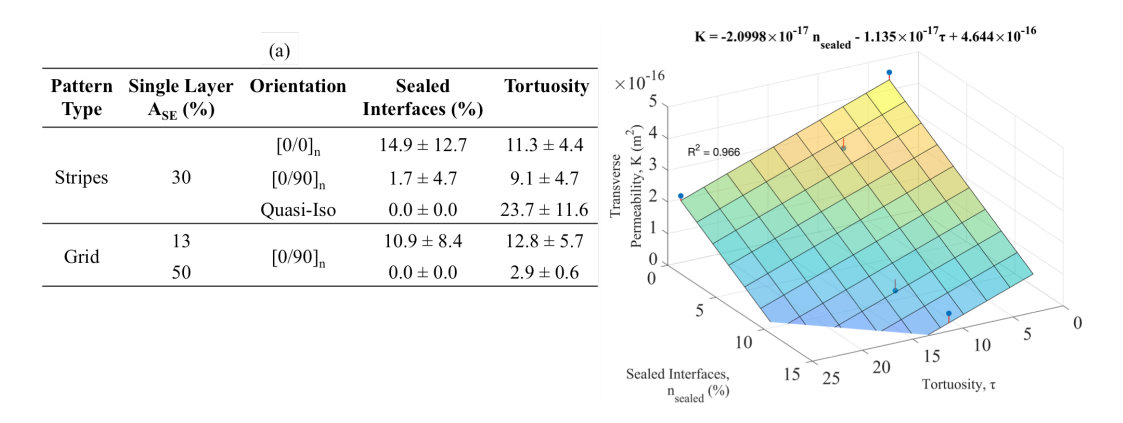


Figure 8. (a) Summary of the sealed interfaces and tortuosity values for each of the 8 ply samples. (b) Transverse permeability values (blue dots) of the tested prepregs and a planar fit (multi-colored plane) via a linear regression model with error bars indicated with red lines.

#### 4. CONCLUSIONS

This work outlines a methodology that allows for rapid evaluation and differentiation of discontinuous resin patterns for VBO prepregs, which can be used to guide prepreg development. The methodology builds on previous work [6,7] that reported a technique to create discontinuous resin patterns of arbitrary shapes and sizes via a polymer film dewetting technique. This technique created a large design space to choose a resin distribution. Without any physical experimentation, the methodology presented here allows one to differentiate between pattern types, feature dimensions, stacking orientations, and ply count.

Various aspects of the optimal design for prepregs with discontinuous resin distribution were outside the scope of this work, although these issues warrant future research. First, this study did not include the changes in bulk factor due to feature dimensions and the subsequent effect on part quality. The bulk factor will be much larger for smaller resin features, however small resin features (large surface openings) will generally result in more efficient air evacuation. Wrinkling in curved surfaces is associated with a large bulk factor, which will decrease the mechanical properties of the composite material. Second, the flow of resin during the cure in relation to maximum feature dimensions was not evaluated. Large surface openings require longer flow distances for full infiltration, which would be more challenging than small surface openings. Understanding the size restrictions with regard to resin flow would be useful to guide future prepreg designs for optimal resin distributions.

Presently, OoA/VBO prepreg processing lacks manufacturing robustness. Often, the manufacturing yields unacceptable defect levels when conditions are not adequately controlled, are non-ideal, or involve complex part geometries. The methods described here provides a pathway to determine favorable and, eventually, optimal designs for prepregs with discontinuous resin distributions. The robustness afforded by the methods presented can, in turn, expand the applicable use of VBO prepregs within aerospace manufacturing and into other non-aerospace applications.

## 5. REFERENCES

- [1] Centea T, Grunenfelder LK, Nutt SR. A review of out-of-autoclave prepregs Material properties, process phenomena, and manufacturing considerations. Compos Part A Appl Sci Manuf 2015;70:132–54. doi:10.1016/j.compositesa.2014.09.029.
- [2] Jackson K, Crabtree B. Autoclave quality composites tooling for composite from vacuum bag only processing. SAMPE Tech Conf, Long Beach, CA: 2002.
- [3] Grunenfelder LK, Dills A, Centea T, Nutt S. Effect of prepreg format on defect control in out-of-autoclave processing. Compos Part A Appl Sci Manuf 2017;93:88–99. doi:10.1016/j.compositesa.2016.10.027.
- [4] Tavares SS, Michaud V, Månson JAE. Assessment of semi-impregnated fabrics in honeycomb sandwich structures. Compos Part A Appl Sci Manuf 2010;41:8–15. doi:10.1016/j.compositesa.2009.09.005.
- [5] Roman M, Howard SJ, Boyd JD. Curable prepregs with surface openings, 2017.
- [6] Schechter SGK, Centea T, Nutt SR. Polymer film dewetting for fabrication of out-of-autoclave prepreg with high through-thickness permeability. Compos Part A Appl Sci Manuf 2018;114:86–96. doi:10.1016/j.compositesa.2018.08.002.
- [7] Schechter SGK, Centea T NS. Fabrication Of Out-Of-Autoclave Prepreg With High Through- Thickness Permeability By Polymer Film Dewetting. Sampe Tech Conf., Long Beach, CA: 2018, p. 2018.
- [8] Helmus R, Hinterhölzl R, Hubert P. A stochastic approach to model material variation determining tow impregnation in out-of-autoclave prepreg consolidation. Compos Part A Appl Sci Manuf 2015;77:293–300. doi:10.1016/j.compositesa.2015.03.021.
- [9] Kompiš V, Qin QH, Fu ZJ, Chen CS, Droppa P, Kelemen M, et al. Parallel computational models for composites reinforced by CNT-fibres. Eng Anal Bound Elem 2012;36:47–52. doi:10.1016/j.enganabound.2011.04.009.
- [10] Centea T, Hubert P. Measuring the impregnation of an out-of-autoclave prepreg by micro-CT. Compos Sci Technol 2011. doi:10.1016/j.compscitech.2010.12.009.
- [11] Al-Raoush RI, Madhoun IT. TORT3D: A MATLAB code to compute geometric tortuosity from 3D images of unconsolidated porous media. Powder Technol 2017;320:99–107. doi:10.1016/j.powtec.2017.06.066.
- [12] Allen TT. Introduction to engineering statistics and six sigma: Statistical quality control and design of experiments and systems. 2006. doi:10.1007/1-84628-200-4.
- [13] Kratz J, Hubert P. Anisotropic air permeability in out-of-autoclave prepregs: Effect on honeycomb panel evacuation prior to cure. Compos Part A Appl Sci Manuf 2013;49:179–91. doi:10.1016/j.compositesa.2013.02.013.
- [14] Tavares SS, Michaud V, Månson JAE. Through thickness air permeability of prepregs during cure. Compos Part A Appl Sci Manuf 2009;40:1587–96. doi:10.1016/j.compositesa.2009.07.004.